

ANTIFERROMAGNETIC RESONANCE OF MANGANESE CARBONATE IN STRONG MAGNETIC FIELDS

L. A. PROZOROVA and A. S. BOROVIK-ROMANOV

Institute of Physics Problems, USSR Academy of Sciences

Submitted June 14, 1968

Zh. Eksp. Teor. Fiz. 55, 1727-1736 (November, 1968)

Both antiferromagnetic resonance branches in MnCO₃ were studied at frequencies from 115 to 170 GHz in magnetic fields up to 50 kOe. The temperature dependence of the energy gap in the high frequency branch of the resonance spectrum, H_{AE}(T), is determined. It is found to be close to the temperature dependence of a weak ferromagnetic moment σ(T). The intersection point of the high and low frequency branches of the spectrum is observed experimentally when H ⊥ z. If H is inclined to the base plane by a few degrees, degeneracy at the intersection point is removed and the shape of the curve depicting the dependence of the resonance frequencies on the field strength indicates the presence of strong interaction between the two oscillation modes. Calculations confirm the regularities observed.

INTRODUCTION

As shown by Turov^[1] and by Borovik-Romanov^[2], in crystals with easy-plane anisotropy (the magnetization of the sublattices is perpendicular to the principal axis of the crystal) with a definite orientation of the magnetic field, the curves describing the dependence of the frequency ν on the field H of the two branches (AFMR) have an intersection point at H ≠ 0 (see Fig. 1). From among the presently known antiferromagnets of this type, MnCO₃, in which the high frequency (HF) branch of the resonance lies in the accessible microwave range (150 GHz) is of greatest interest^[3].

MnCO₃ becomes antiferromagnetic at T = 32.5°K^[2]. As shown by Alikhanov^[4], the magnetization of the sublattices lies in the basal plane. The magnetic structure of this substance is such that, in accordance with the Dzyaloshinskiĭ theory^[5], the moments of the sublattices in the basal plane deviate slightly from strict antiparallel orientation, and produce a weak ferromagnetic moment

$$\sigma = \chi_{\perp} H_D, \tag{1}$$

where χ_⊥ is the susceptibility in the basal plane and H_D is the effective Dzyaloshinskiĭ field (see formula (7)).

Calculation of the dependence of the frequency of both branches of the antiferromagnetic resonance ν on the applied field H^[1,2] has shown that if H ⊥ z, then

$$\nu_1 / \gamma = \sqrt{H(H + H_D)}, \tag{2a}$$

$$\nu_2 / \gamma = \sqrt{H_{AE}^2 + HH_D}, \tag{2b}$$

and if H ∥ z, then

$$\nu_1 / \gamma = 0, \tag{3a}$$

$$\nu_2 / \gamma = \sqrt{H_{AE}^2 + H^2}. \tag{3b}$$

Here γ is the gyromagnetic ratio and H_{AE} is the geometric mean of the exchange field and the anisotropy field.

The low frequency (LF) branch (ν₁) was first ob-

served by Date^[6] and was investigated in detail in^[7], where it was shown that formula (2a) describes well the experimental results if one adds in the right side the term H_Δ² = 1.6/T kOe²/deg, due to the hyperfine interaction, and if one assumes the value H = 4.4 kOe in accordance with the static experiments^[2], and γ = 2.8 (g = 2.0). In^[6,7], the investigations were made in the frequency range from 5 to 40 GHz and in fields from 0.2 to 9 kOe.

Fink and Shaltiel^[3] were the first to observe the HF branch at T = 20.4°K, and Richards^[8] determined the value of H_{AE} = 44.2 ± 1 kOe as T → 0°K.

Figure 1 shows the spectrum of antiferromagnetic resonance at T = 4.2°K, calculated from formulas (2) and (3), using the foregoing values of γ, H_D, and H_{AE}. The purpose of the present work was, first, to study the temperature dependence of H_{AE}, and, second, to investigate the ν(H) dependence near the point of intersection of the two branches¹⁾.

2. PROCEDURE AND SAMPLES

The AFMR line was observed using a simple magnetic spectrometer, the construction of which is de-

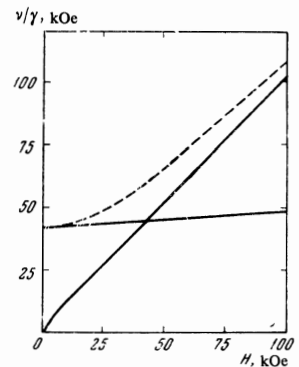


FIG. 1. Spectrum of AFMR in MnCO₃ at T = 4.2°K. Solid curves - H ⊥ z, dashed - H ∥ z.

¹⁾A brief content of the present paper was published in [9].

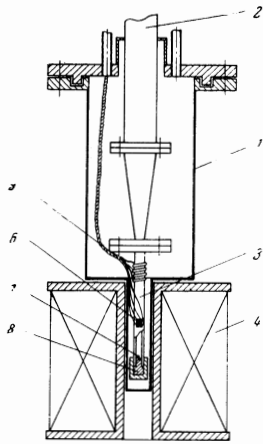


FIG. 2. Diagram of vacuum cryostat: 1 – vacuum jacket, 2 – German silver waveguide with cross section 3.7×7.4 mm, 3 – copper waveguide with cross section 0.8×1.6 mm, 4 – superconducting solenoid, 5 – heater, 6 – resistance thermometer, 7 – sample, 8 – end cap of wave guide.

scribed in^[10]. To obtain temperatures higher than 4.2°K , a vacuum cryostat, shown schematically in Fig. 2, was used. Owing to the vacuum in chamber 1 and the low thermal conductivity of the German silver waveguide 2, the segment of copper waveguide 3 with the investigated sample 7 turns out to be sufficiently well insulated thermally from the surrounding helium bath. Using heater 5, it was possible to maintain the waveguide 3 at any temperature in the interval from 4.2 to $\sim 40^\circ\text{K}$. The temperature was measured with a carbon resistance thermometer graduated at the point 4.2 , 14 , and 20.39°K . The accuracy with which the temperature was measured and maintained was not worse than $\pm 0.2^\circ\text{K}$.

The MnCO_3 single crystals were synthesized by a hydrothermal method by Ikornikova^[11] at the crystallography institute. The main measurements were made on a sample in the form of a cylinder (thickness 0.6 mm, diameter 0.8 mm), the end surfaces of which were natural (111) growth planes. Unfinished crystals were also investigated.

To obtain different sample orientations relative to the applied static field, end caps 8 were used, with different inclinations of the plane to which the sample was glued.

3. HIGH FREQUENCY RESONANCE BRANCH AT $H \parallel z$

By mounting the sample in such a way that the (111) plane was perpendicular to the magnetic field, we observed the absorption line corresponding to the high frequency branch of the spectrum. The measurements were made in the temperature region from 2 to 35°K and at frequencies from 140 to 170 GHz.

A. Temperature Dependence of Line Width

The experimentally observed line half-width ΔH was recalculated in terms of the frequency $\Delta\nu$ by means of the formula

$$\Delta\nu = \frac{2\gamma H}{\sqrt{H_{AE}^2 + H^2}} \Delta H. \quad (4)$$

We have observed that the line width of the AFMR high-frequency branch increases appreciably with decreasing temperature (Fig. 3). This effect depends on the frequency at which the resonance is observed.

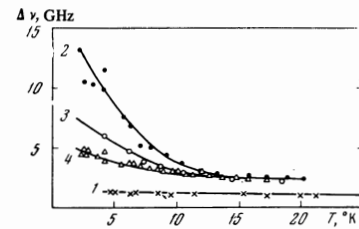


FIG. 3. Temperature dependence of AMFR line width for the LF branch: 1 – $\nu = 10$ GHz, and for the HF branch: 2 – $\nu = 139.7$ GHz, 3 – $\nu = 155.6$ GHz, and 4 – $\nu = 168$ GHz.

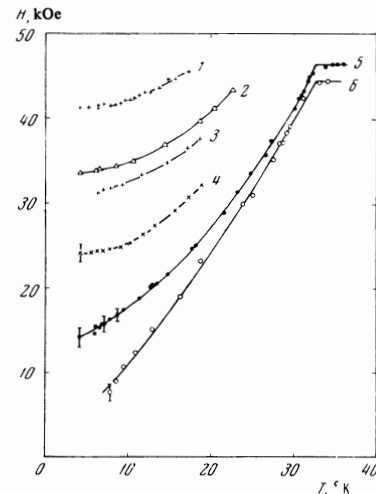


FIG. 4. Temperature dependence of the resonance field ($H \parallel z$) for the following frequencies: 1 – $\nu = 168$ GHz, 2 – $\nu = 155.6$ GHz, 3 – $\nu = 149.8$ GHz, 4 – $\nu = 139.7$ GHz, 5 – $\nu = 130.35$ GHz, 6 – $\nu = 124.2$ GHz.

The increase is particularly large when the frequency is close to γH_{AE} (128 GHz).

It was verified that the line width for the low frequency branch of the AFMR, measured at a frequency 9.4 GHz, as well as at 117 GHz (when $H \perp z$) is practically independent of the temperature (curve 1 in Fig. 3). At high temperatures ($T > 10^\circ\text{K}$), the line widths obtained by us for both branches of the spectrum differ by a factor of 2.

We are unable to present to explain the anomalous growth of the line width for the HF branch. We wish to call attention, however, to the essential difference observed by us between the relaxation mechanisms for the HF and LF oscillation branches at low temperatures.

B. Temperature Dependence of the Gap of High Frequency Branch of AFMR Spectrum

A detailed study of the dependence of the AFMR frequency on the magnetic field was made at a number of temperatures. When plotted in coordinates $(\nu/\gamma)^2$ and H^2 , the experimental points fall on straight lines (see Fig. 3 of^[9]). Our experiments show that $\gamma = 2.8$ (corresponding to $g = 2.00$).

The temperature dependence of the resonant field was investigated at several fixed frequencies. The results are shown in Fig. 4.

Proceeding to discuss the results, we must first

note that the $\nu(H)$ dependence for MnCO_3 agrees, within the limits of our experimental accuracy, with the theoretical formula (3b). The values of H_{AE} were calculated with the aid of this formula from the experimental data. Figure 5 shows the temperature dependence of this quantity. The scatter of the experimental values of H_{AE} at low temperatures is ± 0.4 kOe, which equals ~ 0.1 of the line width. As T_N is approached, the scatter of the points increases as a result of the error in the determination of the temperature. Extrapolation to $T = 0^\circ\text{K}$ yields $H_{AE} = 43.9 \pm 0.2$ kOe. This corresponds to a resonant frequency 123 ± 1 GHz at $T = 0^\circ\text{K}$ and $H = 0$. The same figure shows the values of H_{AE} obtained by other authors. The value obtained by Richards^[8] for $T = 0^\circ\text{K}$ ($H_{AE} = 44.2$ kOe) is close to our result. Fink and Shaltiel^[3] obtained at $T = 20.4^\circ\text{K}$ a value 10% lower

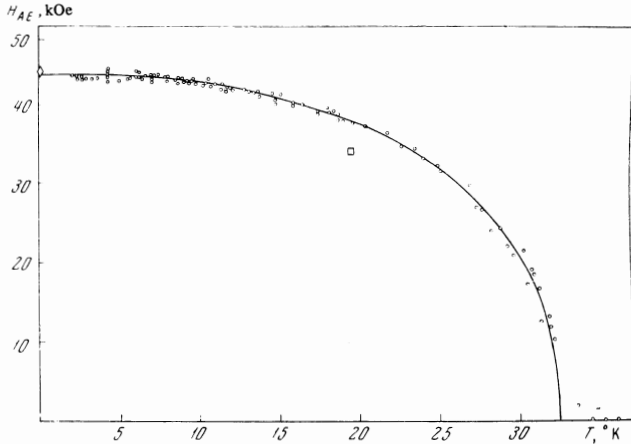


FIG. 5. Temperature dependence of H_{AE} : \diamond — data of Richards^[8], \square — data of Fink and Shaltiel^[3].

than our experimental curve. It is possible that this discrepancy is due to the fact that the crystals used in^[3] had large impurity contents. We have observed that the values of H_{AE} are lower for less perfect crystals.

The question of the temperature dependence of H_{AE} for uniaxial antiferromagnets was discussed in many theoretical and experimental papers (see, for example, the review by Foner^[12]). At the present time the theory cannot predict the temperature dependence of H_{AE} in the entire temperature range from 0°K to T_N . However, within the framework of various theories, it is possible to make some predictions concerning the connection between the temperature dependences of H_{AE} and of the sublattice magnetization \mathcal{M}_0 . The most direct neutron-diffraction data for $\mathcal{M}_0(T)$ are still not accurate enough to be able to use them for such a comparison. An advantage of the substance chosen by us is that it has a weak ferromagnetic moment whose temperature dependence has been thoroughly investigated^[2].

To be able to deduce a connection between $H_{AE}(T)$ and $\sigma(T)$, we write down, following Dzyaloshinskii^[5], an expansion of the thermodynamic potential for crystals with a structure of the MnCO_3 type (group D_{3d}^6) in terms of the components of the unit antiferromagnetism vector $\Lambda = \mathbf{L}/2 \cdot \mathcal{M}_0$ and in terms of the com-

ponents of the magnetization vector \mathbf{M} . These quantities can be regarded as small in the entire region of existence of the antiferromagnetism. Then

$$\Phi(T) = \frac{B(T)}{2} M^2 + \frac{a(T)}{2} \Lambda_z^2 - \beta(T) (\Lambda_y M_x - \Lambda_x M_y) - \mathbf{M} \cdot \mathbf{H}. \quad (5)$$

Here $B(T)$, $a(T)$, and $\beta(T)$ are generally speaking unknown functions of the temperature. Near T_N these functions can be represented in the form of series in powers of the sublattice magnetization, and we can write, retaining the first terms,

$$B(T) = B_0, \quad a(T) = 4a_0 \mathcal{M}_0^2(T), \quad \beta(T) = 2\beta_0 \mathcal{M}_0(T). \quad (6)$$

By minimizing the potential (5) we can easily obtain a connection between the foregoing coefficients and the experimentally measured susceptibility χ_\perp and the weak ferromagnetic moment σ :

$$\chi_\perp = 1/B(T), \quad \sigma(T) = \beta(T)/B(T). \quad (7)$$

Solving the Landau-Lifshitz equation with potential (5) for the AFMR, we obtain formula (3b), with

$$H_{AE}(T) = a(T)B(T). \quad (8)$$

We assume that the formulas in (6) are valid also far from T_N . Then

$$H_{AE}^2(T) = \frac{\beta_0^2}{a_0 B_0^3} \sigma^2(T). \quad (9)$$

Experiment shows that $B = 1/\chi_\perp$ changes very little with temperature. Therefore, if the foregoing assumption is valid, then the temperature dependences of $H_{AE}^2(T)$ and $\sigma^2(T)$ should coincide. Figure 6 shows a comparison of the experimental points obtained by us for the quantity $H_{AE}^2(T)/H_{AE}^2(0)$, and the plots of $\sigma^2(T)/\sigma^2(0)$ taken from^[2] (solid lines). We see that agreement is quite satisfactory. It must be emphasized that complete agreement is obtained from 28°K to T_N , where formula (9) should be exact. The dashed curve in Fig. 6 represents $\sigma^3(T)/\sigma^3(0)$. Such a dependence is predicted for H_{AE}^2 by spin-wave theory at low temperatures (see, for example,^[13]) and by the statistical theory^[14,15] for the entire temperature range. It is seen from Fig. 6 that the dashed curve agrees less well with experiment.

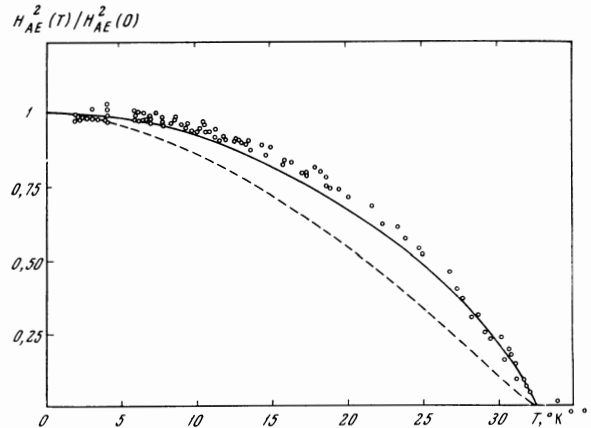


FIG. 6. Comparison of the temperature dependence of the square of the relative magnitude of the gap (experimental points) with the temperature dependence of the relative spontaneous magnetization $\sigma(T)/\sigma(0)$ raised to different powers: solid curve — square, dashed — cube.

4. AFMR SPECTRUM IN THE REGION OF THE INTERSECTION POINT OF TWO BRANCHES

In our first experiments^[16] on the observation of AFMR at $H \perp z$, we operated at a fixed frequency and passed through the region of intersection of the two branches by varying the temperature, since H_{AE} depends strongly on the temperature. It was observed that the results were strongly dependent on the angle α between the field direction and the basal plane. At $\alpha = 0$ only one line of the LF branch was seen, with a position that varied little with temperature. Figure 7 shows plots of the AFMR lines for $\alpha \approx 2^\circ$ at a frequency $\nu = 117.2$ GHz, plotted at temperatures for which $\gamma H_{AE}(T) \approx \nu$. In addition to the AFMR line corresponding to the LF branch, we see here also a line of the HF branch. We see that when the point of intersection is approached the first AFMR line begins to shift and to broaden. These results indicate qualitatively the presence of interaction between the two types of oscillations.

In order to obtain results that can be quantitatively compared with theory, we have plotted, at a fixed temperature, the AFMR spectrum in the vicinity of the intersection point, continuously varying the frequency in the region from 115 to 170 GHz. The results for $T = 4.2^\circ\text{K}$ are shown in Fig. 8. The angle α was determined as follows. After the sample was glued to the end cap, the angle between the (111) plane of the crystal and the end-cap guiding walls entering into the wave guide was measured with a goniometer. The error in the determination of this angle was of the order of $\pm 1^\circ$ and was due mainly to the fact that the guiding walls were not sufficiently flat. Two series of measurements were made, with one sample attachment for which $\alpha = (6 \pm 1)^\circ$. The additional error of 1° could be due to an uncontrollable inclination of the wave guide relative to the solenoid axis. Figure 8 shows the results for $\alpha = (6 \pm 1)^\circ$, and also for $\alpha = (0 \pm 1)^\circ$. At $\alpha = 0^\circ$, it is very difficult to observe the AFMR line of the second branch, since the field dependence of the frequency is very weak here. Therefore Fig. 8 shows the theoretical straight line for this branch.

The results give grounds for the following conclusion. When the field is exactly perpendicular to the z axis, there is practically no interaction between the two oscillation modes; there is a point of intersection of the two branches, i.e., at a definite value of the magnetic field the spectrum of the spin-system oscillations has a degeneracy. When the field is inclined to the basal plane, a coupling arises between the oscillations, the degeneracy is lifted, and a characteristic distortion of the plots of the resonance frequency against the magnetic field is observed.

The qualitatively obtained results can be explained by considering the magnetic symmetry of MnCO_3 . In the absence of the magnetic field, or when the field is directed along the binary axis or the symmetry plane, the magnetic symmetry groups consist respectively of the following elements^[5]:

$$C_2, I, \sigma_d \text{ or } C_2R, I, \tilde{\sigma}_dR. \quad (10)$$

It is easy to show that all the components Λ_i and M_k are divided into two groups:

$$M_y, M_z, \Lambda_x \text{ and } \Lambda_y, \Lambda_z, M_x; \quad (11)$$

These two triads of variables are transformed in accordance with different irreducible representation of the symmetry groups (10). We can therefore conclude immediately that these variables should separate in the equations of motion, and their oscillations should not interact. If the field is taken out of the plane, then the magnetic group contains only one element \tilde{I} , with respect to which all 6 components are transformed in the same manner and the constraint on the entangling of the variables is lifted.

For a quantitative description of the observed form of the AFMR spectrum, we write down the equations of motion for the unit vector of the antiferromagnetic moment Λ and for the vector of the magnetic moment M . The Landau-Lifshitz equations for the sublattices can be readily transformed into

$$\begin{aligned} \frac{1}{\gamma} \frac{\partial \Lambda}{\partial t} &= \left[\Lambda \frac{\partial \Phi}{\partial M} \right] + \frac{1}{4M^2} \left[M \frac{\partial \Phi}{\partial \Lambda} \right], \\ \frac{1}{\gamma} \frac{\partial M}{\partial t} &= \left[\Lambda \frac{\partial \Phi}{\partial \Lambda} \right] + \left[M \frac{\partial \Phi}{\partial M} \right]. \end{aligned} \quad (12)$$

In our case the expression for Φ is of the form (5). However, in order not to present cumbersome formulas, we shall henceforth assume that $\beta = 0$. Such an approximation is valid, since H_D is much smaller than the external field near the point of intersection and the field H_{AE} . We introduce the amplitudes of small oscillations of the vectors Λ and M , namely λ and μ respectively. Linearizing the system (12), we obtain

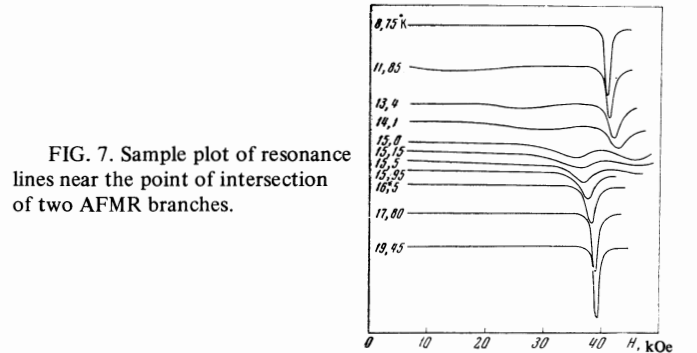


FIG. 7. Sample plot of resonance lines near the point of intersection of two AFMR branches.

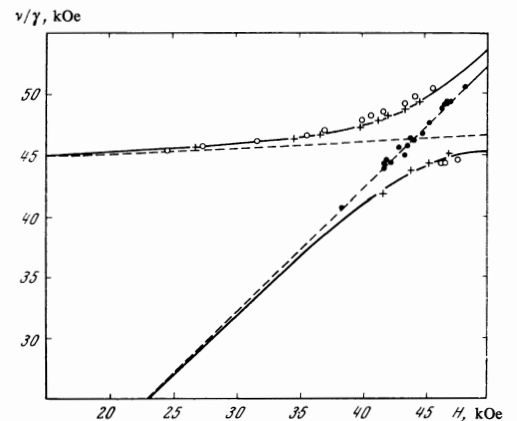


FIG. 8. AFMR spectrum near the intersection point: + and O — two series of measurements with $\alpha = 6^\circ$, · — measurements with $\alpha = 0$. The dashed lines are plots of formulas (2a) and (2b), and the solid lines are the results of calculation for $\alpha = 7^\circ$ using equation (16)

for an antiferromagnet with easy-plane type of anisotropy ($a > 0$):

$$\begin{aligned} \frac{i\nu}{\gamma} \lambda_x &= -B\mu_z, & \frac{i\nu}{\gamma} \lambda_y &= \frac{aH}{B\beta\mu_0^2} \lambda_z, \\ \frac{i\nu}{\gamma} \mu_y &= -M_z B\mu_x + H\mu_z, & \frac{i\nu}{\gamma} \lambda_z &= B\mu_x, \\ \frac{i\nu}{\gamma} \mu_z &= -H\mu_y, & \frac{i\nu}{\gamma} \mu_x &= M_z B\mu_y - a\lambda_z. \end{aligned} \quad (13)$$

Here $M_Z = HB^{-1} \sin \alpha$. In accordance with the foregoing symmetry considerations, the equations in (13) break up when $\alpha = 0$ into two independent systems. Each of these systems contains variables of only one of the triads. In oscillations of the first branch, with frequency

$$\nu_1 = \gamma H \quad (14)$$

only the first triad of components changes. The frequency of the second branch is in our approximation

$$\nu_2 = H_{AE}. \quad (15)$$

At this frequency, oscillations of the second triad take place. When $\alpha \neq 0$, all the equations become coupled and we obtain for the frequencies of the coupled oscillations the following equation:

$$\nu^4 - \nu^2(\nu_1^2 + \nu_2^2 + \gamma^2 H^2 \sin^2 \alpha) + \nu_1^2 \nu_2^2 = 0. \quad (16)$$

Here ν_1 and ν_2 are solutions of (14) and (15) when $\alpha = 0$. As seen from (13), the coupling between the two oscillation modes is produced by the magnetization component M_Z . The foregoing calculation shows that the coupling constant contains the product of M_Z by the exchange coefficient B . As a result, the coupling turns out to be unexpectedly large.

We have also performed the calculation for the case when $\beta \neq 0$. For the condition $H \gg \alpha\beta/4B\beta\mu_0^2$ and $H_D \ll H_E$, which is realized in practice, we obtained in this case equation (16) in which ν_1 and ν_2 are the solutions (2a) and (2b) when $\alpha = 0$. The solid curves of Fig. 8 were obtained from the values of $\nu(H)$ calculated from (16) with $\alpha = 7^\circ$. If we take into account the statements made above concerning the accuracy with which α is determined, we can assume that the agreement between calculation and experiment is good. Thus, the appearance of the magnetization component M_Z leads to coupling between the two oscillation modes.

In conclusion, attention must be called to the fact that, from the point of view of symmetry, interaction can arise also when $\alpha = 0$, if the field is inclined away from the rotational direction. In this connection, we have verified whether lifting of the degeneracy occurs when the direction of the field is changed in the basal plane. It was established that, within the limits of our measurement accuracy, there is no lifting of degeneracy in the case when the field H is directed in the basal plane along the bisector of the angle between the two-fold axis and the line of intersection with the symmetry plane.

5. CONCLUSION

We investigated in this paper AFMR in $MnCO_3$ at frequencies 115–170 GHz and obtained the following basic results:

1. It was shown that the dependence of the frequency of the HF branch of the AFMR on the magnetic field

applied along the trigonal axis, at all temperatures from 2.5°K to $T_N = 32.5^\circ K$, has the theoretically predicted form $\nu/\gamma = \sqrt{\frac{H_{AE}^2}{\gamma^2} + H^2}$.

2. An anomalous growth of the AFMR line width was observed when the temperature was decreased below 10°K. This growth was observed only for the HF branch of the AFMR.

3. The temperature dependence of $H_{AE}(T)$ was determined and was shown to be close to the temperature dependence of the weak ferromagnetic moment.

4. The value $H_{AE}(0^\circ K) = 43.9 \pm 0.2$ kOe was obtained.

5. It was shown that if the field lies in the basal plane, then a point of degeneracy of the two branches of the AFMR spectrum exists at $H \neq 0$. The degeneracy is lifted if the field is directed away from the basal plane.

6. The dependence of the frequencies of both branches of the AFMR spectrum on the magnetic field was calculated near the point of their intersection at a field inclined to the basal plane. Good agreement between the calculated and experimental curves was obtained.

The authors thank P. L. Kapitza for interest in the work, I. E. Dzyaloshinskiĭ for useful discussions, N. Yu. Ikoznikov for supplying the $MnCO_3$ single crystals. We are grateful to K. I. Rassokhin and V. S. Zakizov for help with the experiments.

¹E. A. Turov, Zh. Eksp. Teor. Fiz. 36, 1255 (1959) [Sov. Phys.-JETP 9, 890 (1959)].

²A. S. Borovik-Romanov, Zh. Eksp. Teor. Fiz. 36, 766 (1959) [Sov. Phys.-JETP 9, 539 (1959)].

³H. J. Fink and D. Shaltiel, Phys. Rev. 130, 627 (1963).

⁴R. A. Alikhanov, Zh. Eksp. Teor. Fiz. 36, 1690 (1959) [Sov. Phys.-JETP 9, 1204 (1959)].

⁵I. E. Dzyaloshinskiĭ, Zh. Eksp. Teor. Fiz. 32, 1547 (1957) [Sov. Phys.-JETP 5, 1259 (1957)].

⁶M. Date, J. Phys. Soc. Japan, 15, 2251 (1960).

⁷A. S. Borovik-Romanov, N. M. Kreĭnes, and L. A. Prozorova, Zh. Eksp. Teor. Fiz. 45, 64, (1963) [Sov. Phys.-JETP 18, 46 (1964)].

⁸P. L. Richards, J. Appl. Phys. 35, 850 (1964).

⁹A. S. Borovik-Romanov and L. A. Prozorova, Trudy Mezhdunarodnoĭ konferentsii po fizike nizkikh temperatur (Proceedings of the Tenth International Conference on Low Temperature Physics) 4, VINTI, Moscow 1967, p. 201.

¹⁰G. D. Bogomolov, Yu. F. Igonin, L. A. Prozorova, and F. S. Rusin, Zh. Eksp. Teor. Fiz. 54, 1069 (1968) [Sov. Phys.-JETP 27, 572 (1968)].

¹¹N. Yu. Ikoznikova, Kristallogr. 6, 745 (1961) [Sov. Phys.-Crystallogr.]

¹²S. Foner, Antiferromagnetic and Ferrimagnetic Resonance, in: "Magnetism", 1, Academic Press, New York, (1963), p. 383.

¹³T. Oguchi, Phys. Rev. 113, 769 (1959).

¹⁴N. S. Akulov, Z. Physik, 100, 197 (1936).

¹⁵C. Lener, Phys. Rev. 96, 1335 (1954).

¹⁶A. S. Borovik-Romanov and L. A. Prozorova, ZhETF Pis. red. 4, 57 (1966) [JETP Lett. 4, 39 (1966)].